ELSEVIER

Nuclear Instruments and Methods in Physics Research A 427 (1999) 455–464

NUCLEAR INSTRUMENTS & METHODS IN PHYSICS RESEARCH Section A

A cryogenic current-measuring device with nano-ampere resolution at the storage ring TARN II

T. Tanabe[a,*], K. Chida[a], K. Shinada[b]

[a]*High Energy Accelerator Research Organization, Tanashi, Tokyo 188, Japan*
[b]*Keihanna Research Laboratory, Shimadzu Co., 3-9 Hikaridai, Seika-cho, Kyoto 619-02, Japan*

Received 29 September 1998

Abstract

In cooler-ring experiments, an accurate and non-destructive current measurement is essential for determining the reaction cross sections. The lowest current which can be measured by the DC current transformer commonly used so far is some μA. In order to measure a low-beam current from nA to μA, we made a cryogenic current-measuring device using a superconducting quantum interference devices (SQUID), and measured the circulating ion current at the cooler ring TARN II. This paper gives the design and performance of the device.

PACS: 07.20.Mc; 07.55.Nk; 29.20.Dh; 41.85.Ew

Keywords: Storage ring; Beam current; Cryogenic device

1. Introduction

Atomic-physics experiments on the electron–ion collision processes have been extensively performed on heavy ions, molecular ions and negative ions at storage rings with electron cooling. One important result concerning physics is the absolute values of the cross sections, for which accurate intensity measurements of ion beams are required without interfering with the circulating ion beams in the ring. Under the typical experimental conditions, the circulating beam is cooled by electron cooling [1], and the cooled beam is usually not bunched, but coasting. Therefore, it is necessary to measure the DC current. A standard current-measuring device which has been widely used so far in circular accelerators is the DC current transformer (DCCT), the sensitivity of which is some μA. On the other hand, the intensities of the ion beams used in atomic-physics studies at storage rings, such as molecular ions, are mostly below the lowest measurable limit by the DCCT. Furthermore, such ions are fragile, and their lifetimes are typically a few seconds. The intensities are supposed to be from some nA to some μA for these ions [2]. A new type of beam-intensity monitor using a SQUID was designed in order to non-destructively measure

* Corresponding author. Tel.: +81-424-69-9565; fax: +81-424-68-5543.

E-mail address: tanabe@tanashi.kek.jp (T. Tanabe)

0168-9002/99/$ - see front matter
PII: S0168-9002(99)00058-3

low-intensity ion beams circulating in the ring. The SQUID is an extremely sensitive magnetic sensor, which means that it is easily affected by any external magnetic background. The application of a SQUID to beam-current measurements was reported by Grohmann et al. [3] and Peters et al. [4]. However, this device has not yet been designed for use in ion-current measurements at storage rings, where the following problems peculiar to these rings must be solved: a large-size warm bore, compatibility with the ultra-high vacuum of the beam pipe, fitting to a narrow space, shielding against high-level electro-magnetic noise and mechanical vibration. The device was designed while considering these problems. The system was installed in the storage ring TARN II [5] at the high energy accelerator research organization and measurements were carried out for molecular ions. This paper describes the design and performance of the device.

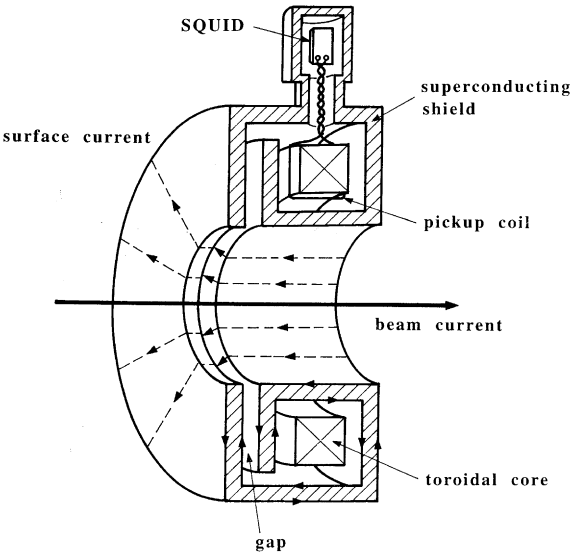

Fig. 1. Principle of the cryogenic current-measuring device.

2. Design of the cryogenic current-measuring device

2.1. Principle of the cryogenic current-measuring device

The design of the cryogenic current-measuring device is based on cryo-current comparators (CCC). Since the underlying principle of the CCC has been described by Grohmann et al. [3,6], we give only a brief summary here. The principle is shown in Fig. 1. The detection area is protected by a superconducting magnetic shielding. The beam current induces an azimuthal magnetic-field component, which turns on a surface current on the superconducting shielding according to Meissner effect. Since the shielding is not closed, but has a gap, the inner and outer regions are coupled by the surface current on the shielding. The gap plays the role of filtering; the azimuthal magnetic-field component with information about the beam current can enter the shielding without attenuation, while the other field components are strongly attenuated. The magnetic field induced by the surface current can then be detected by a pickup coil surrounding a toroidal core with high permeability. The important thing is that the net surface current is equal to the total beam current flowing through the bore of the shielding and is independent of the beam's location. Since the pickup coil is coupled to a SQUID, the current through the pickup loop turns on a magnetic field in the SQUID, which is detected by the SQUID circuit.

2.2. SQUID and driving circuit

For the SQUID system, a double washer DC SQUID with direct feedback coils is used, which has been developed as a magnetic flux sensor for a multi-channel biomagnetometer [7]. Fig. 2 shows a circuit diagram of a SQUID with direct feedback coils and a flux-locked loop. The magnetic field inside the superconducting shield induced by the surface current is transformed to a current of the pickup coil by the toroidal core, which acts as a flux-coupling transducer. Since the loop from the pickup coil to the input coil of the SQUID via the coupling coil is superconductive, the induced current flows in the input coils without attenuation, which turn on the flux in the SQUID. The SQUID output is amplified by the room-temperature circuit and is fed to feedback coils, which produce a magnetic flux in the coupling coils. This flux cancels the signal current flowing through the

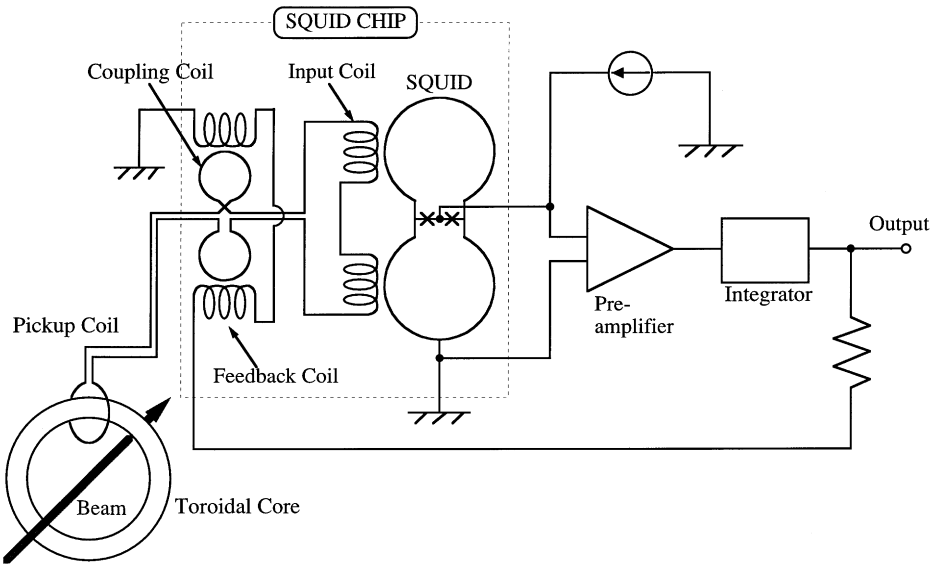

Fig. 2. Circuit diagram of the double-washer SQUID with direct feedback coils and a flux locked loop.

Table 1
Electrical parameters of the SQUID circuit at liquid-helium temperature

SQUID inductance	125 pH
Input coil inductance	200 nH
Feedback coil inductance	200 nH
Pickup coil inductance (at room temperature)	125 μH
Mutual inductance between SQUID and input coil	5 nH
Mutual inductance between feedback coil and coupling coils	6 nH

coupling coils, so as to keep the SQUID output constant. Since the feedback coils do not couple to the SQUID, but directly couple to the coupling coils, current flowing in the pickup-input coil loop can be avoided. This feature is especially favorable for multi-channel use, because the magnetic field, which can affect other coils as cross talk, does not exist. With this flux-locked loop, good linearity for a wide dynamic range was realized. Various electrical parameters relating to the circuit are listed in Table 1.

In order to remove any stray field penetrating the circuit, a double-washer structure is adopted in both the SQUID loops and the coupling coil loops. When a uniform magnetic field penetrates a pair of washer coils, inverse currents are generated in these coils, resulting in canceling each other. Josephson junctions made by focused ion-beam technology have some special features. They are very short and weak links, which exhibit good reproducibility and durability against both temperature and humidity [7]. A SQUID chip made by using the photolithography process is shown in Fig. 3. The total white-noise level, including pre-amplifier noise, is $2\text{–}4\times10^{-6}\phi_0/\sqrt{\text{Hz}}$, where ϕ_0 is a flux quantum.

2.3. Magnetic shielding and flux-coupling coil

The magnetic shield has to meet the demand that the azimuthal magnetic-field component can enter into the shielding with small attenuation, while the other field components are strongly attenuated. Various types of superconducting magnetic shielding have been studied relating to the CCC. Among them, a folder-type structure (as schematically shown in Fig. 1) comprising several ring cavities [6] was chosen due to its narrow width and easy manufacturing procedure. In this type of shielding, the

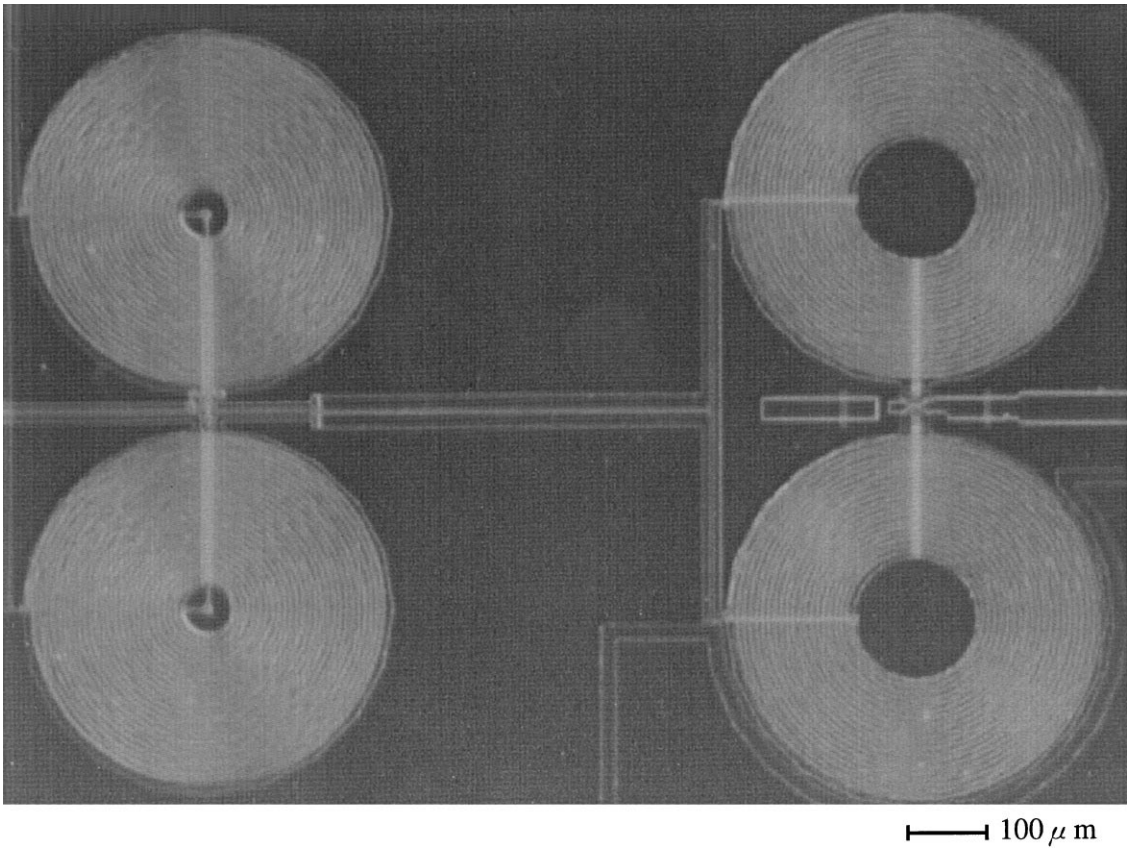

Fig. 3. Double-washer DC SQUID with input coil (right) and feedback coil with coupling coil (left).

shielding efficiency increases along with an increase in the ratio of the outer radius to the inner radius and with number of cavities [6]. If the inner radius is fixed, the increase in the shielding efficiency inevitably leads to an increase in weight. Since the shield is made of lead, the weight increases steeply with the shielding efficiency. Prior to the design, a small test device [8] was made and some fundamental tests were made with it, which included the sensitivity, shielding efficiency from an external field, zero drift and noise. We designed the shielding having eight ring cavities as shown in Fig. 4, taking into account the allowable size and weight, while also referring to the shielding efficiency during a model test. The shield was made by cutting and welding lead sheets having a thickness of 3 mm. A gap with a thin width of 0.5 mm between the lead sheets was isolated with Teflon sheets. The weight of the shield is about 20 kg.

For the complete magnetic shielding, even pin hole in the shield had to be avoided. However, there is a hole for cables on the top of the SQUID housing. In order to shield the external magnetic field entering from this hole, the cables from the SQUID are inserted in a thin and long lead pipe which is shaped in a meandering structure.

In order to ensure strong coupling of the magnetic flux, a toroidal core was used. The core needs to have a high permeability and a low noise figure at liquid-helium (L-He) temperature. The noise figure is especially important, because the resolution is mostly determined by the noise level. However, data on the noise figure at the L-He temperature is scarce, and is also unpredictable from that at room

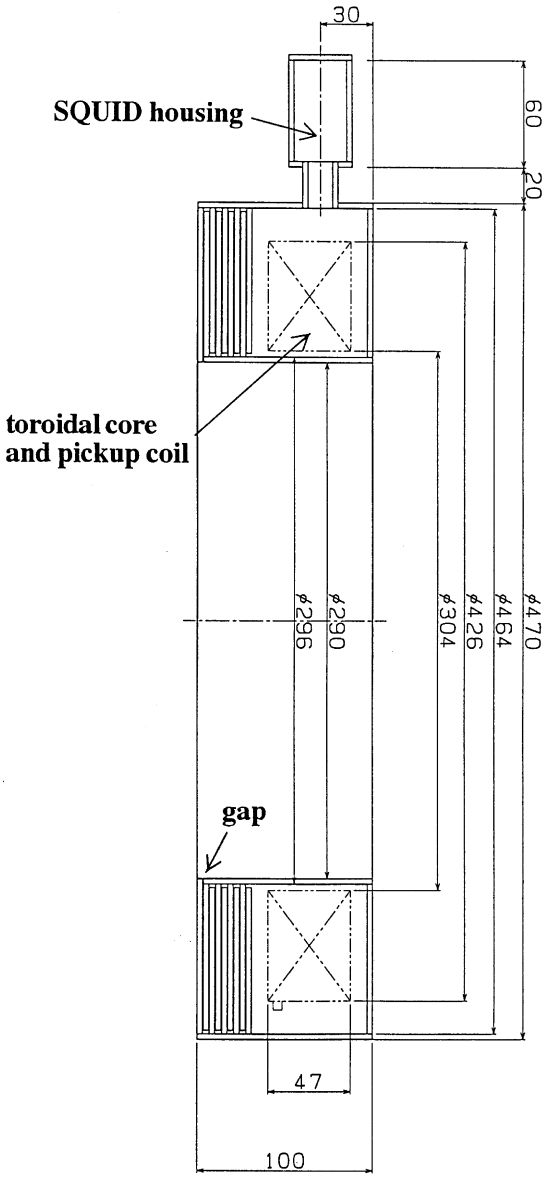

Fig. 4. Design sketch of magnetic shield. Sizes are indicated in unit of mm.

temperature. Therefore, several types of toroidal cores consisting of amorphous alloy and nanocrystal alloy were tested in our model studies; "VITROVAC 6025F" (Vacuumschmelze GmbH, Germany) was chosen, since it showed the lowest noise figures at L-He temperature. The dimensions of the toroidal core are as follows:

Inner diameter: 322 mm,
Outer diameter: 400 mm,
Width: 25 mm.

Since a toroidal core with high permeability is used, the sensitivity of the SQUID decreases along with an increase in the number of turns of the pickup coil. Therefore, one turn is chosen for the pickup coil. In order to distribute the coil along the circumference of the core, a one-turn coil was designed to comprise a Nb toroid having a slit along the circumference housing the toroidal core. The inductance of the pickup coil at room temperature is 125 μH, which decreases by a factor of about four at L-He temperature. Although the inductance is still much larger than that of the input coil, the SQUID sensitivity is sufficiently high for our present purpose, as described later.

2.4. Cryostat

The cryostat consists of a vacuum isolation chamber and a L-He container in which the detector system is immersed. The cryostat is shown in Fig. 5. In order to use L-He effectively, the center of the detector system is offset from that of the L-He container. The total width is designed to be only 50 cm, in order to match the limited space reserved for this device in the storage ring. The inner diameter of the beam pipe is 16 cm, which is large enough for the passing ion beam. The vacuum of the vacuum isolation chamber ($\sim 10^{-7}$ Torr) is much inferior to that of the beam pipe of the ring (typically 10^{-11} Torr). Therefore, the vacuum of the beam pipe is isolated from that of the cryostat, so as not to affect the ultra-high vacuum of the ring. All the vacuum components are made from low-magnetic permeability material of 316L stainless steel. To avoid any wall currents induced by the ion beam, ceramic isolating pipes are inserted into both the beam tube and the liquid-helium container tube. The ends of ceramic pipes were vacuum-sealed with non-magnetic cupro-nickel instead of Kovar, which is a magnetic substance. Inside the vacuum isolation chamber, there is a copper radiation shield, which is cooled by a cryo-refrigerator at a temperature of around 40 K. The whole copper

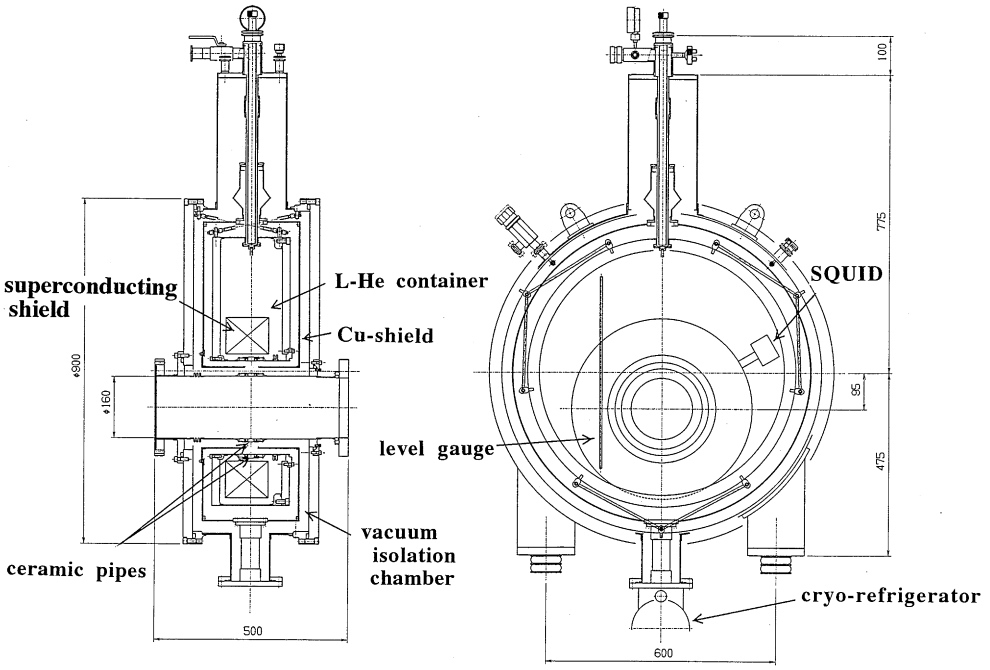

Fig. 5. Design of the cryostat for the cryogenic current measuring device. Sizes are indicated in unit of mm.

shield is wrapped up in superinsulation foils. In order to avoid heat conduction, the L-He container is suspended by two thin titanium rods and also reinforced by FRP (fiber reinforced plastic) rods from the side walls. With this system a holding time of 1 day was achieved with an effective liquid-helium stock volume of 30 l. The L-He consumption rate is about 20 l/d.

Low-frequency noise due to mechanical vibration seriously deteriorates the resolution of the system. In order to isolate the device from vibration of the floor, it was installed on four rubber bearings. Furthermore, thin-walled metal bellows on each side of the device dampen vibrations from the beam pipe at both ends. Since the refrigerator is a type having low-mechanical vibration, it was unnecessary to stop it during measurements. The total weight of the cryostat, including the magnetic shield and toroidal core, is about 700 kg. The device installed at the center of one of the six straight sections in the TARN II ring is shown in Fig. 6.

3. Experimental results

The output signal is sent to the counting room 50 m apart from the device by way of a isolation amplifier. The output voltage was then digitized by an A/D converter and stored in a computer every 0.1 s. The ion beam is simulated with a one-winding wire loop around the magnetic shielding. Fig. 7 shows the output of the SQUID electronics as a function of the calibration current of the ion-beam simulation loop. A good linearity was obtained up to 2.5 μA. The current sensitivity was 5 mV/nA, which is high enough to measure current of the order of nA. Calibrations with a simulated current were performed for two one-turn windings around the magnetic shielding; one along the beam axis and the other the off axis and close to the magnetic shielding. Both results agree well within the experimental errors, which ensures that the output does not depend on the beam's location.

To search for the background source, the noise spectrum of the output signal was measured using

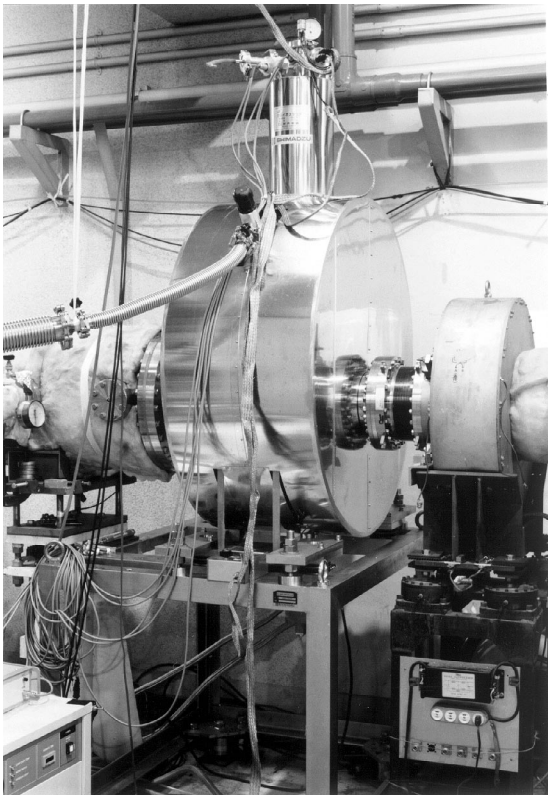

Fig. 6. Cryogenic current measuring device installed at the TARN II ring.

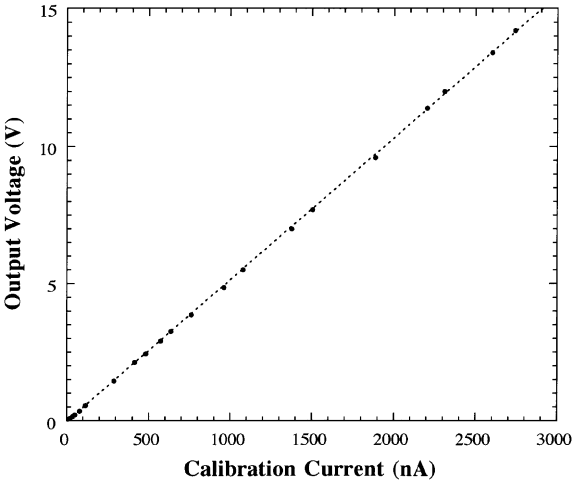

Fig. 7. Current calibration data. Dots represent experimental data.

a spectrum analyzer. As can be seen in Fig. 8, low-frequency noise between 10 and 20 Hz is highest and limits the resolution. It probably comes from mechanical vibration originating from many rotary pumps working in the TARN II room.

The shielding efficiency was tested by adding uniform external magnetic fields with Helmholtz coils wound outside of the cryostat. An external field ($\boldsymbol{B}$) of 10^{-5} T parallel or perpendicular to the beam current ($\boldsymbol{I}$) yields the following apparent currents:

$\boldsymbol{B} \| \boldsymbol{I} \sim 4$ nA

$\boldsymbol{B} \perp \boldsymbol{I} \sim 80$ nA.

In order to raise the shielding efficiency even more against any external magnetic field, the entire system was covered with Permalloy-metal with a thickness of 1 mm. According to a calculation, an additional increase in the shielding efficiency by a factor of about 10 is expected. Although there are many normal- and super-conducting magnets and an RF system in the TARN II room, the system was not affected even during operation of the whole system.

At the beginning of cooling, the output of the SQUID system showed a strong zero drift. The drift rate gradually decreased with time. After cooling for 2 days, the zero drift dropped to values under 0.5 mV/s (0.1 nA/s current drift). Although we repeated a heat cycle between 4 and 80 K several times, depending on the experimental schedule, no strong drift was observed. Although the reason for the drift is not clear, it surely originates in the toroidal core.

Fig. 9 shows the output voltages with a series of 10 nA-10 s test pulses. The voltage from the SQUID circuit was filtered by a low-pass filter with a frequency of 10 Hz, and was then fed to an A/D converter. As can be seen in the figure, a sensitivity of 1 nA was achieved. A typical example of measurements with a 14 MeV HD^+ ion stored in the TARN II ring is given in Fig. 10. The current increases abruptly during injection (about 200 μs), and then gradually decreases with time due to

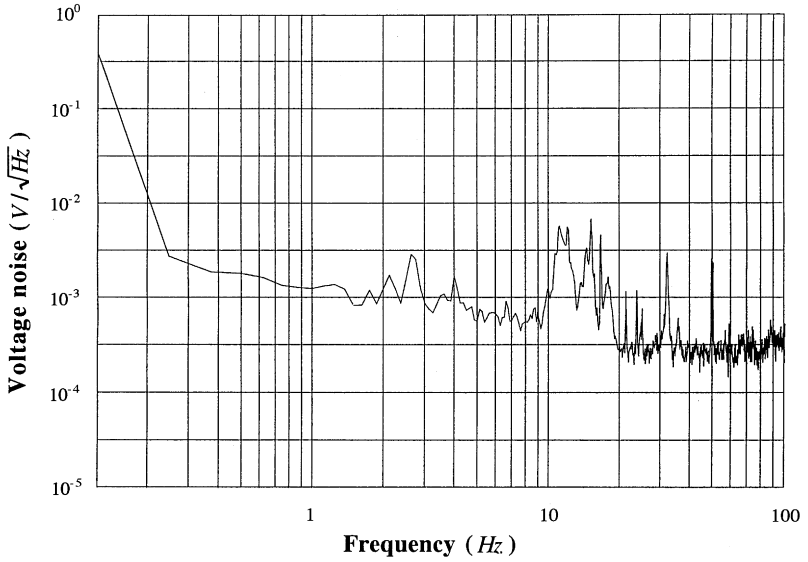

Fig. 8. Noise spectrum.

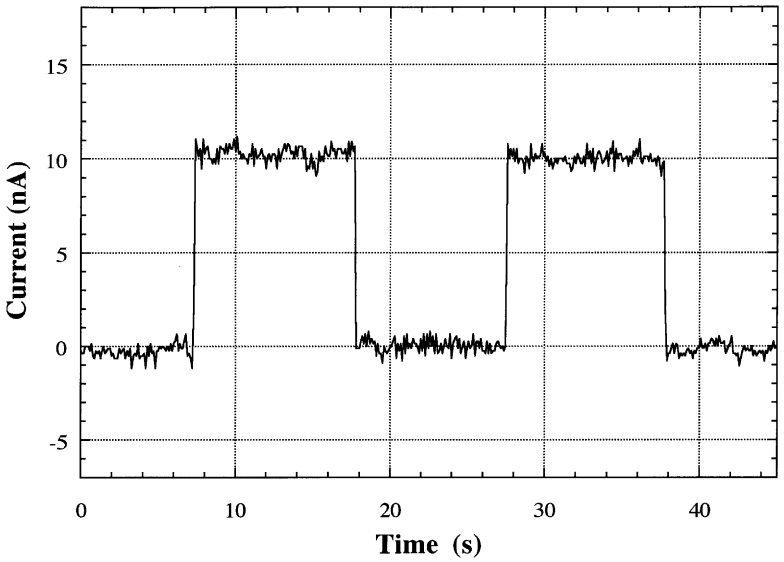

Fig. 9. Output for the 10 nA–10 s pulse current.

dissociation of the molecular ion caused by collisions with the residual gas molecules. The discrete change in the current at the low level in the figure is due to the resolution of the 12-bit A/D converter for this measurement (the data in Fig. 9 was taken with a 16-bit A/D converter). When the noise level exceeds the slew rate of the measuring system, the feedback circuit of the SQUID becomes unstable and unlocked. Such unlocking occurs every few hours.

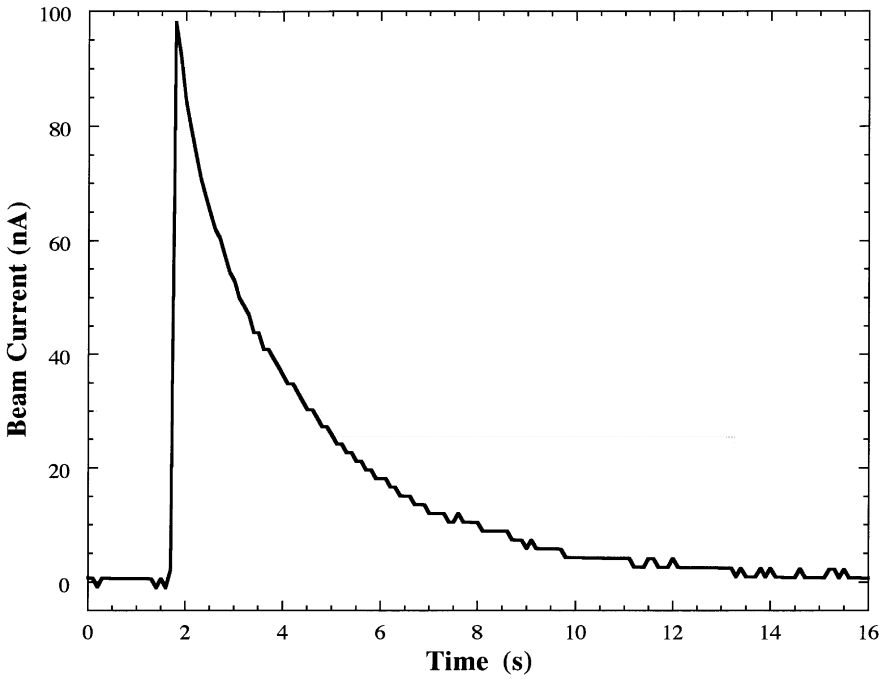

Fig. 10. Measured ion current stored in the TARN II. The current decreases due to dissociation of the molecular ion HD^+.

4. Conclusion

Accurate nondestructive current measurements are essential to determine the cross sections in atomic-collision experiments in cooler rings. The most ambiguous quantity in determining the cross sections is the beam current. Despite the importance of current measurements, there has so far been no device to measure a low-DC beam current below some μA. Under these circumstances, the development of a current-measuring device with high sensitivity has been desired for a long time. Although the principle of the cryogenic current measuring device is simple, an actual device is not so easy to construct. Problems related to the storage ring were solved by the present experiments. The device is expected to contribute to the determination of a basic physical quantity, the cross section. The device is now working as a powerful tool for determining absolute cross sections for the atomic-physics experiments at TARN II.

Acknowledgements

The author (T.T.) is grateful to A. Peters of GSI for valuable discussions on the device. The authors thank H. Okubo of Suzuki Shokan Co. for constructing of the cryostat and Y. Yamada of Shimadzu Co., K. Hatanaka and Y. Sasaki of Osaka Univ. and S. Ono of Univ. of Tokyo for their helpful collaborations concerning the model test. They also thank T. Fujino, Y. Funahashi and T. Norimatsu of the machine shop of KEK for the machining and welding the Nb cavity, M. Yoshizawa of KEK for the data processing and members of the TARN II group for their interests.

References

[1] T. Tanabe, K. Noda, T. Honma, M. Kodaira, K. Chida, T. Watanabe, A. Noda, S. Watanabe, A. Mizobuchi, M. Yoshizawa, T. Katayama, H. Muto, A. Ando, Nucl. Instrum. and Meth. A 307 (1991) 7.

[2] T. Tanabe, I. Katayama, S. Ono, K. Chida, T. Watanabe, Y. Arakaki, Y. Haruyama, M. Saito, T. Odagiri, K. Hosono, K. Noda, T. Honma, H. Takagi, J. Phys. B 31 (1998) L297.
[3] K. Grohmann, D. Hechtfischer, J. Jakschik, Superconducting Quantum Interference Devices and their Applications, Walter de Gruyter, Berlin, 1977, p. 311.
[4] A. Peters, H. Reeg, C.H. Schroeder, W. Vodel, H. Koch, R. Neubert, H. Mühlig, Proceedings of the fifth European Particle Accelerator Conf., Sitges, 1996, Institute of Physics Publishing, p. 1627.
[5] T. Katayama, K. Chida, T. Hattori, T. Honma, M. Kanazawa, A. Mizobuchi, M. Nakai, A. Noda, K. Noda, M. Sekiguchi, F. Soga, T. Tanabe, N. Ueda, S. Watanabe, T. Watanabe, M. Yoshizawa, Proceedings of the 14th International Conference on High Energy Accelerators, Tsukuba, 1989, Particle Accelerators 32 (1990) 105.
[6] K. Grohmann, H.D. Hahlbohm, D. Hechtfisher, H. Lübbig, Cryogenics, 16 (1976) 423; Cryogenics, 16 (1976) 601.
[7] K. Shinada, T. Munaka, M. Ueda, Y. Fujiyama, S. Nagamachi, Y. Yamada, Proceedings of the fifth International Superconductive Electronics Conference, Nagoya, 1995, p.364.
[8] T. Tanabe, S. Ono, T. Watanabe, K. Hatanaka, Y. Sasaki, Proceedings of the XVI RCNP Osaka International Symposiom on Multi-GeV High-Performance Accelerators and Related Technology, Osaka, 1997 World Scientific, Singapore, p.247.